TABLE III. Comparison of the observed transition probabilities with calculated transition probabilities for the 246 and 46.7 keV $E2$ transitions.

Energy (keV)	Angular momentum Initial	Final	$P_{(obs)}$(sec^{-1})	P_{sp}(sec^{-1})[a]	P_{coll}(sec^{-1})[b]
246	4	2	$3.1\pm0.4\times10^8$	0.272×10^8	0.412×10^8
46.7	6	4	$5.4\pm0.7\times10^4$	0.264×10^4	[c]

[a] Interacting particle calculations using the wave functions from Ref. 5.
[b] Collective calculations using the wave functions from Ref. 6.
[c] Wave function for the 6^+ level were not available in (6).

states shows some improvement over the other, which includes configuration mixing effects only. The 46.7-keV transition probability as calculated, including only configuration mixing effects, is not in as good agreement as that of the 246-keV transition.

There is still an enhancement factor unaccounted for. This enhancement may be explained through a recent approach,[18] which employs a modified Brueckner-Gammel-Thaler[19] two nucleon potential in the determination of the configuration mixing for the first excited states of Po^{210}. Another possibility, under present investigation, is that of a pairing interaction effect,[20,21] in the quasiparticle approximation.

Note added in proof. Since the submission of this paper, Kim and Rasmussen[22] have published wave functions for Po^{210} and computed $E2$ transition probabilities using an effective charge of $1.814e$. In our calculations, the effective charge is taken to be $1.002e$. The values of the ratio $P(E2)_{obs}/P(E2)_{cal}$ for the 246-keV transition are 11.4, 7.5, and 11.2 using the wave functions of Newby and Konopinski, Guman *et al.*, and Kim and Rasmussen, respectively.

ACKNOWLEDGMENTS

The authors wish to express their sincere gratitude to Milan Oselka and his co-workers at the Argonne National Laboratory 60-in. cyclotron, for their invaluable aid in the irradiation of the bismuth targets. Special thanks are due to William R. Haller of the Notre Dame Chemistry Department for his efforts in the source handling. We also wish to thank Dr. H. J. Prask, Dr. J. J. Reidy, and J. F. McNulty for their help in accumulation of the data.

[18] Y. E. Kim and J. O. Rasmussen, University of California, Radiation Laboratory Report UCRL-10624 **A24**, 1962 (unpublished), p. 69.
[19] K. A. Bruechner and J. L. Gammel, Phys. Rev. **109**, 1023 (1956).
[20] M. Baranger, Phys. Rev. **120**, 459 (1960).
[21] S. Yoshida, Nucl. Phys. **38**, 380 (1962).
[22] Y. E. Kim and J. O. Rasmussen, Nucl. Phys. **47**, 184 (1963).

PHYSICAL REVIEW VOLUME 132, NUMBER 6 15 DECEMBER 1963

Absolute Positive Pion Photoproduction Cross Sections from Hydrogen*

R. J. WALKER,† T. R. PALFREY, JR., R. O. HAXBY, AND B. M. K. NEFKENS‡
Department of Physics, Purdue University, Lafayette, Indiana
(Received 5 August 1963)

Absolute differential cross sections for the photoproduction of pions of 33.8-MeV laboratory kinetic energy from protons were measured at eight angles between 29.5 and 146.1° in the center-of-mass system. The over-all absolute accuracy is 4%, while the relative accuracy within the angular distribution is 3%. Comparison is made to various theoretical calculations, with and without inclusion of the effect of a γ-π-ρ-meson coupling. Existing calculations based on dispersion theory give only fair agreement with the data.

I. INTRODUCTION

DURING the past several years considerable refinement has been achieved in the theory in the theory of the reaction

$$\gamma+p\rightarrow\pi^++n$$

at energies below the $T=\frac{3}{2}$, $J=\frac{3}{2}$ resonance. Arguments based on dispersion theory, such as those of Chew, Goldberger, Low, and Nambu[1] lead to detailed predictions for the absolute differential cross sections in terms of the pion-nucleon scattering phase shifts, and the pion-nucleon coupling constant. Ball,[2] and more recently McKinley,[3] have attempted to introduce the effect of a γ-π-ρ-meson coupling into dispersion-theory calculations. The new theoretical work encouraged this attempt

* Supported in part by the U. S. Atomic Energy Commission.
† Present address: Physics Department, Northwestern University, Evanston, Illinois.
‡ Present address: Physics Department, University of Illinois, Champaign, Illinois.

[1] G. F. Chew, M. L. Goldberger, F. E. Low, and Y. Nambu, Phys. Rev. **106**, 1345 (1957), referred to as CGLN throughout the text.
[2] J. S. Ball, Phys. Rev. **124**, 2014 (1961).
[3] C. S. Robinson, P. M. Baum, L. Criegee, and J. M. McKinley, Phys. Rev. Letters **9**, 349 (1962). This letter provides further references to University of Illinois Technical Reports in which the theoretical work of McKinley is given in detail.

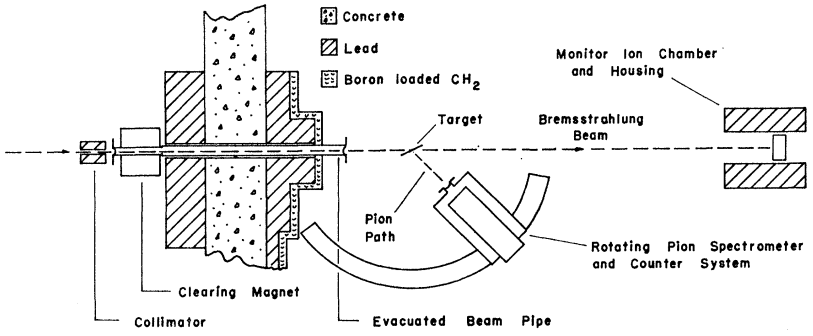

FIG. 1. Plan view of experimental arrangement.

for a statistically and systematically improved measurement of the absolute differential cross section for single positive pion photoproduction in the region of 200-MeV energy.

Previous absolute measurements in the energy region of this experiment[4–12] have been taken under a variety of conditions and with a number of differing techniques. Comparison is made to some of these results in Sec. IV.

The basic technique used in the experiment reported here was to detect pions of a fixed energy as a function of angle with a counter and magnetic spectrometer system of known acceptance. Bremsstrahlung photons were used as the gamma-ray source, with two-body kinematics giving the incident photon energy in terms of the laboratory pion energy and angle.

Certain features of the design of the experiment reported here need introductory comment:

1. The differential cross sections were measured at constant laboratory pion energy. Consequently, each point in the angular distribution corresponds to a different center of mass energy. In particular, the laboratory photon energy varies in these measurements from 185 to 230 MeV. Comparison to theory is still possible, of course. The alternative procedure of holding fixed the center-of-mass energy leads to a variation of pion energy with angle in the laboratory, and consequently, to systematic variations of experimental conditions with angle, and thus reduces the relative accuracy of data obtained in this way.

2. The absolute acceptance of the spectrometer was measured as a function of source position with a source emitting alpha particles of the same $H\rho$ as the pions.

3. The peak bremsstrahlung energy was varied with pion angle in such a way that $\bar{k}/k_0$, the ratio of the average energy of the photon producing the counted pions to the peak bremsstrahlung energy, was held constant. This procedure serves two purposes: It helps reduce the variation of the muon contamination with angle. (This is because a significant fraction of the counted muons come from pions of higher energy than those counted, and these pions, in turn, come from the part of the bremsstrahlung above the part used in producing the counted pions.) In the second place, this procedure uses the same relative portion of the bremsstrahlung spectrum at all angles, so that uncertainties—which indeed exist—in the shape of the spectrum will contribute only to the absolute accuracy, and not significantly to the relative accuracy.

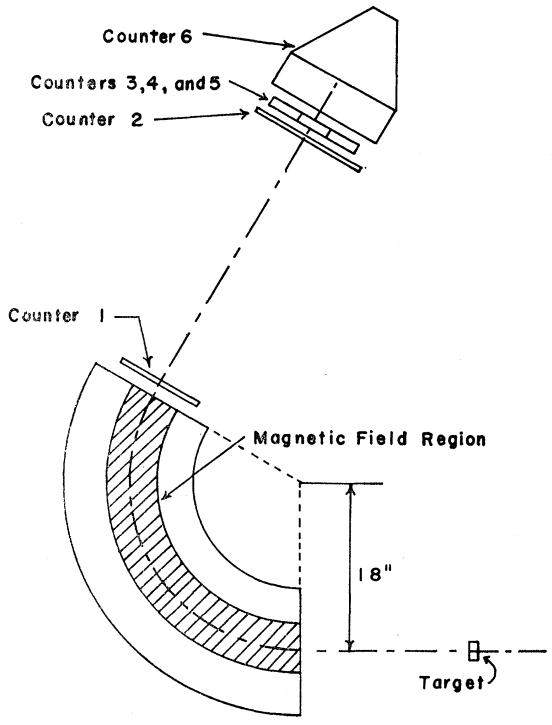

FIG. 2. Side view of detection equipment, showing outline of magnetic spectrometer and cross-section view of target and counters.

[4] M. Beneventano, G. Bernardini, D. Carlson-Lee, G. Stoppini, and L. Tau, Nuovo Cimento **4**, 323 (1956).
[5] T. L. Jenkins, D. Luckey, T. R. Palfrey, and R. R. Wilson, Phys. Rev. **95**, 179 (1954).
[6] J. Steinberger and A. S. Bishop, Phys. Rev. **86**, 171 (1952).
[7] G. Bernardini and E. L. Goldwasser, Phys. Rev. **94**, 729 (1954).
[8] A. V. Tollestrup, J. C. Keck, and R. M. Worlock, Phys. Rev. **99**, 220 (1955).
[9] G. M. Lewis, R. E. Azuma, E. Gabathuler, D. W. O. S. Leith, and W. R. Hogg, Phys. Rev. **125**, 378 (1962).
[10] G. S. Janes and W. L. Kraushaar, Phys. Rev. **93**, 900 (1954).
[11] J. K. Walker and J. P. Burq, Phys. Rev. Letters **8**, 37 (1962).
[12] G. M. Lewis, D. W. G. S. Leith, D. L. Thomas, R. Little, and E. M. Lawson, Nuovo Cimento **27**, 384 (1963).

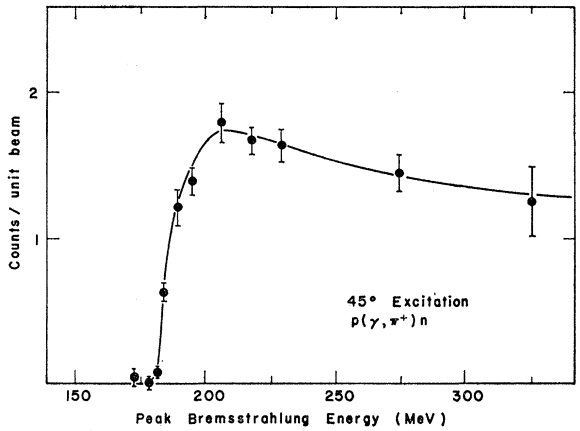

FIG. 3. Yield of π^+ from protons as a function of peak-bremsstrahlung energy. Units of the yield are proportional to the pions/joule of incident beam.

4. Muon contamination and multiple scattering out of the detection system—the two largest systematic corrections required in the reduction of the data—were both checked by experimental measurements.

II. EXPERIMENTAL ARRANGEMENT AND PROCEDURE

The basic experimental arrangement is depicted in Figs. 1 and 2. The component parts are described in the subsections below.

A. The Gamma-Ray Beam

The photon beam was produced by bremsstrahlung of electrons from the Purdue synchrotron on an internal 0.040-in. Pt. wire target whose axis is parallel to the electron-orbit axis. The beam was spread to a width of 500 μsec and centered in time on the peak of the sinusoidal guide-field wave form of the synchrotron, the half-period of which was about 15 msec. The γ rays were collimated 1.50 m from the internal target to a rectangular shape, 1.2-cm wide by 1.7-cm high. After collimation the beam entered a vacuum pipe, passed through the field of a clearing magnet and through a lead, barite-loaded concrete, and boron-loaded paraffin shielding wall. The beam struck the meson-producing target at 4 m from the internal bremsstrahlung target, and was monitored by a Cornell-type ionization chamber[13] at 7 m from the internal target.

The spacial distribution of the gamma intensity across the target influences the pion source distribution. This, in turn, affects the relationship between counting rate and cross section through the spacial dependence of the spectrometer acceptance. The γ-ray spacial distribution was obtained from $C^{12}(\gamma,n)C^{11}$ activation measurements as a function of peak-bremsstrahlung energy.

[13] F. J. Loeffler, T. R. Palfrey, and G. W. Tautfest, Nucl. Instr. and Methods 5, 50 (1959).

Peak-bremsstrahlung energy was determined for this experiment in terms of the spectrometer magnet calibration with alpha particles. The calibration source was Po^{210}, so that the alpha-particle trajectories in the system are the same as those for pions of about 31-MeV kinetic energy, or for positrons of about 99.5-MeV/c momentum. These kinematics were used to obtain two reference peak-bremsstrahlung points by pion photoproduction, and one by electron-pair production, as follows:

1. At laboratory angles of 45 and 135°, the spectrometer was used to measure the yield of 31-MeV pions from protons as a function of peak-bremsstrahlung energy. The 45° yield curve is shown in Fig. 3. The 45 and 135° pion-excitation functions established the monitor calibration to an accuracy of ± 1 MeV at 185 and at 230 MeV, respectively.

2. The spectrometer was used at 0° to measure the end point of the positron spectrum from electron-pair production. This established a calibration point in the neighborhood of 100-MeV photon energy, well below any of the running energies; this calibration indicated adequate linearity of the energy monitor from 100 to 230 MeV.

During the running the peak-bremsstrahlung energy was set at 1.15 times the mean photon energy responsible for production of the detected pions at each angle, and was maintained to about 0.3%.

B. Targets

The meson-producing targets were plane slabs of Polyethylene and graphite, the thicknesses of which were chosen to keep the pion energy loss the same in both targets. The CH_2-C subtraction was chosen for three reasons: experimental ease and simplicity, the precision of positioning possible with plane targets, and the fact that at low-photon and low-pion energies (particularly at forward angles) carbon is a relatively ineffective source of pions because of binding energy effects. Over the entire angular range, the ratio of counts from H_2 to counts from C in the polyethylene target lay between 1.0 and 2.0.

Orientation of the targets varied with pion angle, the criterion for angular positioning being that the pion-source width as seen by the spectrometer be held constant. As a consequence the target thickness, both in pion direction and in photon direction, varied by $\pm 15\%$ between angles. These variations were systematically accounted for in the data reduction.

C. The Meson Spectrometer Magnet

The meson spectrometer is a 120°, $n=0.5$, 18 in. mean radius, 2-in. $\times$ 5-in. aperture double-focussing magnet. Mesons were produced at a mean distance of 18 in. from the entrance edge of the pole pieces, and the detection plane used was normal to the central orbit, 33 in. from the exit edge of the poles. This detector

position lies closer to the exit edge of the magnet than does the true focal plane of the spectrometer.

The region between the poles was evacuated. During the alpha-particle acceptance measurements the entire system, from source to detector, was evacuated.

The spectrometer acceptance was calibrated with alpha-particles from an electrodeposited Po^{210} source. The detector, a ZnS screen viewed by a single photomultiplier, was identical in size to the scintillation counters used to count the pions. It was positioned in each of the three momentum-channel positions subsequently used in the pion experiment. For each of these detector positions the source was moved over a three-dimensional grid somewhat larger than the final meson-producing targets. At each grid position, the acceptance of the spectrometer (i.e., the decay-corrected alpha-particle counting rate) was measured as a function of the spectrometer momentum setting. The absolute acceptance was determined from the counting rate by the insertion of known aperture-defining stops at the entrance to the spectrometer. Counting statistics were better than 1% at all points near maximum acceptance, with corresponding accuracy along the wings of the curves. As an example, one such acceptance curve is given in Fig. 4. It was taken at the central target position, and is for the central momentum channel.

To analyze the pion data it was convenient to Fourier-fit the magnet acceptance curves, and then to develop power series of the Fourier coefficients in Cartesian coordinates about the central point of the target. This permits ready computer calculation of the absolute pion yield from each volume element of any arbitrarily shaped target contained in a 2 in. cube centered on the central target position. Errors in the fits contribute no more than a 1% uncertainty to the cross section.

D. Counters and Electronics

The counter system can be seen in Fig. 2. Counters $C1$ and $C2$ are plastic scintillators 0.65 g/cm² thick. These intercept all of the pions going to the momentum-defining counters $C3$, $C4$, and $C5$, each of which is a 2.6 g/cm² plastic scintillation counter, Counter $C6$ is a Lucite Čerenkov anticoincidence counter, sensitive to electrons but not to the slow pions (or muons) emerging from the momentum-defining counters.

Each counter signal was fed directly into a transistorized, beam-gated discriminator circuit. A scalar drive output from each of these circuits permitted continuous monitoring of singles rates in all counters. The discriminator module also provided output pulses to drive the 30 nsec coincidence and anticoincidence circuits. Scalers read the 12, 16, and $12\bar{6}$ coincidence rates, in addition to the pion rates $123\bar{6}$, $124\bar{6}$, and $125\bar{6}$. An independent signal channel was available from each of the counters, one at a time, so that pulse-height distributions could be inspected. An example of such a distribution is given in Fig. 5, and the bias level at which the discriminator

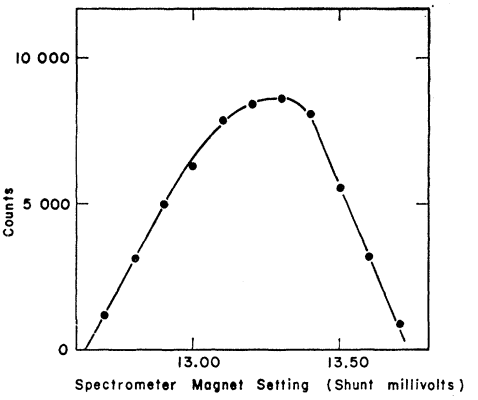

FIG. 4. Alpha-particle calibration data for spectrometer acceptance of a single momentum channel for a single source position. "Counts" on the abscissa are proportional to steradians.

was set is indicated on the figure. The bias is set to include all of the pions and some of the accompanying muons. Biases on each of the counters in turn were set with mesons. The Čerenkov counter bias was adjusted at a forward angle with a mixed pion and electron beam from a lead target.

The combination of pulse-height requirements in the scintillation counters and the Čerenkov anticoincidence gave the system a measured net 0.02% efficiency for electron detection, and reduced electron background to a completely negligible level. Discriminator biases and counter thickness removed a fraction of the muon counts and are together largely responsible for the fact that, although about 35% of the pions decay in flight in the system, the counted muon contamination is only about 5% of the counted pion rate. Protons or other heavier charged particles originating in the target have insufficient range to penetrate the counter telescope after momentum selection.

Singles rates were of the order of 10^3 to 10^4 counts/sec during beam spill-out. Counting losses and chance coincidence rates were negligible at all angles.

E. Running Procedure

Once biases had been established in all the discriminators, a ThC″ gamma-ray source was used daily in standard geometry to check counter operation. During the running no counter or logic circuit failed or drifted significantly. The C and CH_2 targets were alternated about once per hour, and the pion angle was changed every few hours during a total run of several hundred hours. Running times at each angle were set to yield the same statistical accuracy in the subtraction. An independent beam-monitoring thin-walled ionization chamber was used at all times as a check on the operation of the standard monitor. Potentiometric checks of the spectrometer magnet current setting and of the synchrotron energy setting were taken regularly. Pressure and temperature were recorded with each angle

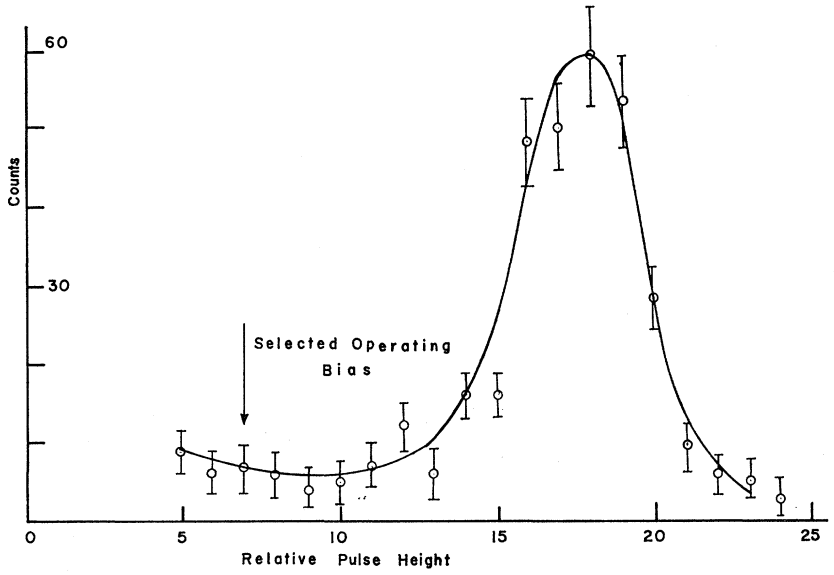

FIG. 5. Pulse-height distribution in momentum channel counter 4 for particles meeting pion logic requirements in counters 1, 2, and 6.

change to obtain the necessary small corrections to the collected charge from the ionization chambers. A series of runs was taken without any pion-producing target (other than air) in the beam. The target-out rates, about 1% of the target-in rates, were subtracted appropriately.

F. Multiple Scattering Measurements

Counter $C1$ was physically separated from the rest of the telescope, as can be seen in Fig. 2. This choice of geometry reduces the 12 coincidence rate and thus the chance triples rates. The negative effect of the separation is that $C1$ introduces a significant multiple-scattering loss of the pions going through the telescope. This effect can be crudely calculated, but a precise description of the flux of pions incident on the counter is lacking, and this lack prevents a precise calculation of the effect of multiple scattering. However, the effect was measured, as follows:

Positrons of the same $p\beta$ as the pions were counted (with coincidence requirements 236, 246, and 256) with and without counter $C1$ in place, and with a series of absorbers placed in the position of $C1$. (The use of positrons was necessary to obtain sufficient counting rate for an accurate measurement.) Counting losses were thus measured directly, and the variation of counting loss with the thickness of $C1$ in radiation lengths was obtained. The measured counting loss was 9%, while a crude calculation gave 8%.

G. Muon Contamination Runs

It is convenient to think of two components of the muon flux: muons arising from the decay of pions which would have been counted in the detection system, had they not decayed, and muons from other pions. The counting efficiency for the former class is small because of the decay-in-flight kinematics, the biases in the counters, and the range restriction of the telescope. The counting-rate contribution of this class can therefore be calculated with sufficient accuracy, and is actually less than 1% of the counted pion rate.

Muons coming from the decay of other pions mostly originate in the region near the target and in the first half of the spectrometer magnet. They are therefore moderately well resolved in momentum, and could, in principle, be separated on the basis of a precise range curve. The counting rates were not sufficiently high for a good range curve, so the contamination from this second class of muons was determined by the following indirect technique:

First, the Čerenkov counter $C6$ was replaced by a large scintillation counter in which the momentum-resolved muons would stop and in which a delayed pulse from μ-e decay could be observed. This, by itself, does not measure the contamination, because nearly every stopping π^+ will also give rise to a delayed e^+ through the $\pi^+ \rightarrow \mu^+ \rightarrow e^+$ sequence. This fact, however, was used to obtain a good measure of the detection efficiency of the counter for μ-e decay, as follows: The spectrometer field was increased until positive pions came to rest with essentially the same range distribution in the new counter $C6$ as the momentum-resolved contamination muons of the pion production runs. Inspection of the time distribution of delayed pulses from the new $C6$, triggered by any of the coincidences 123, 124, or 125, showed that the counter detected muon decay positrons with efficiencies in the neighborhood of 80%.

The next step was to reverse the spectrometer field and measure negative pions from a Be target. Delayed μ-e events in this arrangement are a direct measure of muon contamination, because the stopped negative

pions are essentially all captured before decay. (A small correction was made for muon capture in the scintillator C6.)

These data, with the additional assumption that the μ^- contamination in the π^- beam is the same as the μ^+ contamination in the π^+ beam, are sufficient to yield a good value for the contamination. These measurements were performed for each of the momentum channels, and at several angles.

Muon contamination from all sources was $4\pm1\%$ and was independent of angle.

III. TREATMENT OF DATA

The yield of pions from protons at each angle θ, $Y(\theta)$, can be expressed as an integral over photon energy k and target coordinates x, y, and z, in the following way:

$$Y(\theta)=A\int\int\int dxdydz\int NEFW(d\Omega^*/d\Omega)(d\sigma/d\Omega^*)dk.$$

The inner integral is over photon energy k from zero to the peak-bremsstrahlung energy k_0. The outer integral is a volume integral over the meson-producing target.

The constant A includes such quantities as the target thickness, the response of the gamma-ray beam monitor, corrections for nuclear attenuation, muon contamination, and multiple scattering quantities either independent of or only weakly dependent on the integration variables.

$N=N(k,k_0)$ represents the gamma-ray spectrum. In particular, it is chosen half-way between the Schiff integrated-over-angles distribution and the distribution integrated up to an angle of $4mc^2/k_0$.[14]

$E=E(p')$ represents the survival probability of a pion of momentum p' through the detection system. The momentum p' is related to the momentum of the pion at production, p, and, hence, to the energy of the photon creating the pion, by application of ordinary ionization energy-loss expressions to the pion between its creation in the target and entry into the spectrometer vacuum system.

$F=F(x,y)$ is an appropriately normalized function giving the distribution of intensity in the gamma-ray beam in the plane normal to the gamma-ray direction z.

$W=W(x,y,z;p')$ is the known acceptance solid angle of the spectrometer.

The quantity $d\Omega^*/d\Omega$ is the usual kinematic transformation of solid angle between the center-of-mass and laboratory systems. Its small dependence on pion angle was suppressed in the calculations, leaving only the dependence on photon energy k, because the acceptance aperture of the spectrometer is only 3°.

The cross section to be determined, $d\sigma/d\Omega^*$, is a function of k and θ. Again the small dependence on angle was suppressed in the calculation. The energy dependence of $d\sigma/d\Omega^*$ was obtained from CGLN, and is sufficiently good for use in the calculation.

[14] H. W. Koch and J. W. Motz, Rev. Mod. Phys. **31**, 920 (1959).

TABLE I. Cross-section results.

C.m. angle (degrees)	Cross section (μb/sr)
29.5	7.73±0.23
39.8	7.67±0.23
54.8	7.33±0.22
71.3	7.76±0.23
88.8	8.81±0.26
106.9	9.81±0.29
125.3	11.44±0.34
146.1	12.36±0.37

Every quantity in the integration is thus known except for the magnitude of the cross section. This is chosen to make the calculated yield agree with the experimental yield, and it is this value of the cross section which is quoted in Sec. IV.

Because the momentum acceptance of the spectrometer is nearly 15%, it is also necessary to determine the energy at which to quote the experimental results. To do this we weight the integrand of $Y(\theta)$ by T, the pion kinetic energy at production, integrate, and take the ratio of the energy-weighted yield to the unweighted yield. This ratio gives the appropriate pion kinetic energy at which the results of the experiment should be compared to theory.

The calculations described in this section were evaluated for each angle on an IBM-7090 computer. Hand calculations verified the operation of the computer program. Subsidiary computer runs verified the necessity for keeping particular functions under the integral, or justified their removal, and determined the mesh size needed for the various integrations.

IV. RESULTS AND ERRORS

The results of the measurements are given in Table I and in Fig. 6. The curves shown with the data points in Fig. 6 are discussed in Sec. V.

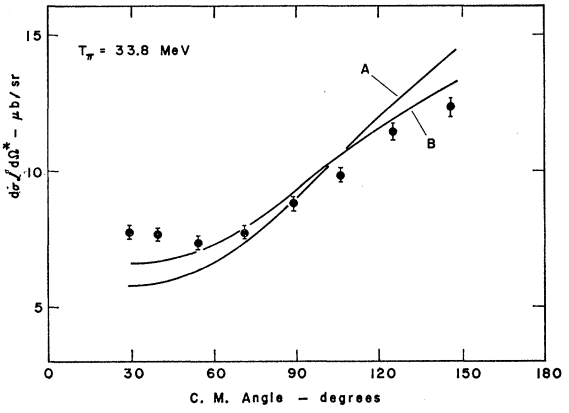

FIG. 6. Experimental results. Curves are explained in Sec. V of text.

TABLE II. Absolute error contributions.

Effect	Error
1. Bremsstrahlung intensity monitoring	3%
2. Spectrometer acceptance	2%
3. Bremsstrahlung spectrum shape	1%
4. Counter edge effects	1%
5. Muon contamination	1%
6. Multiple scattering	0.6%
7. Pion lifetime	0.5%
8. Peak bremsstrahlung energy	0.5%
9. Other errors, total	~1.1%
Total	4.2%

The relative errors in the angular distribution are dominated by the statistical errors, which are about 3%.

The absolute error in the cross section, i.e., the factor by which one could raise or lower all of the eight points together, is about 4%, and comes from a large number of sources. The principal sources of error, in decreasing order of importance, are shown in Table II.

It should be noted that errors numbered 1, 3, 8, and part of 9 have to do with problems connected with the gamma-ray beam rather than the detection apparatus, and contributed about two-thirds of the mean-squared error.

Errors 5 and 7, having to do with pion decay in flight, are nearly independent. The former has to do with the measurement of the relatively small muon contamination triggering the electronics, and the latter comes from present uncertainties in the pion lifetime.

Comparison of the results of this experiment to results obtained in other laboratories is made in Fig. 7. The points with solid-error flags are taken directly from experiments, and the errors are as given in the original sources. (The data of Tollestrup *et al.*[8] have been raised by 7% to correct for monitor differences discussed in Ref. 4.) The points shown with dotted-error flags are small energy interpolations of the results of other experiments. In these cases the assigned errors are merely meant to be indicative of the errors in the neighboring points in the original source.

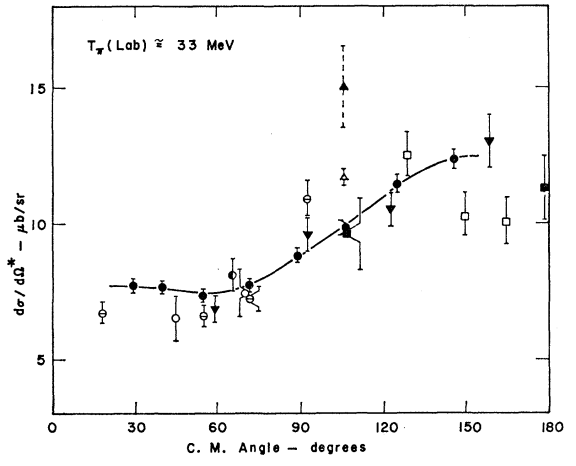

FIG. 7. Comparison to other measurements. The key to the points is: • Present result; ▼ Beneventano *et al.* (Ref. 4); ■ Jenkins *et al.* (Ref. 5); △ Steinberger and Bishop (Ref. 6); □ Tollestrup *et al.* (Ref. 8); ⊖ Lewis *et al.* (Ref. 9); ▲ Janes and Kraushaar (Ref. 10); ○ Walker and Burq (Ref. 11); and ◐ Lewis *et al.* (Ref. 12).

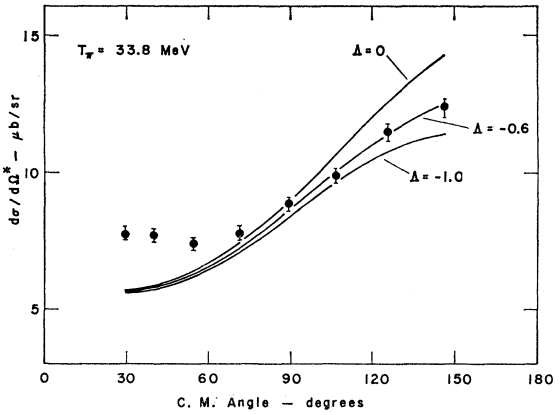

FIG. 8. Comparison of experimental results to predictions calculated from the theory of McKinley (Ref. 3). Curves are explained in text.

We note consistency with the more recent data, i.e., that of Beneventano *et al.*,[4] Lewis *et al.*,[9,12] and Walker and Burq.[11]

V. DISCUSSION OF RESULTS

An effort was made to compare the results to the theoretical predictions of CGLN, in the use of which a number of different choices of pion-nucleon phase shifts were tried. At these energies relatively small differences show up between results calculated with differing reasonable choices of phase shifts. Consequently, we present as a typical example, a comparison of the results of this experiment with CGLN using $f^2=0.08$ and, for phase shifts, the "Set X" of McKinley given by Robinson *et al.*[3] Figure 6 shows these results as curve A. Somewhat better agreement with the experimental results is obtained by use of the theoretical phase shifts of CGLN.[15] These are shown as curve B in Fig. 6. Neither curve A nor curve B gives adequate agreement with the experimental results. However, curve B is mostly within the 5–10% accuracy hoped for by Chew *et al.*[1]

The recent good success of Robinson *et al.*[3] in explaining the results of a 43-MeV pion angular distribution measurement with a particular dispersion theory calculation incorporating the effect of a γ-π-ρ coupling prompted us to attempt to fit our results with the same parameters. Briefly, the parameters used here are: $f^2=0.08$, McKinley's "Set X" phase shifts, a ρ-meson mass of 735 MeV, and the CGLN electric dipole term $N^{(-)}$ set equal to zero. One is then free to vary the strength of a γ-π-ρ coupling constant Λ here expressed

[15] G. F. Chew, M. L. Goldberger, F. E. Low, and Y. Nambu, Phys. Rev. **106**, 1337 (1957).

in units of electron charge e. In order to make a fair comparison, the method of McKinley[3] was used to calculate the result, rather than the method of CGLN. Except for the ρ-meson mass, these are the same parameters used by Robinson *et al*; the effect of changing the mass is quite small, and nearly equivalent to a small change in coupling constant Λ.

Figure 8 shows the result of our McKinley-type calculation for three different values of Λ. No normalization has been made. It is indeed true that the agreement at backward angles is better for small negative values of Λ, as in the results of Robinson *et al.* However, the absolute value of the cross section is in disagreement with our results for as large a value of Λ as -1.0. Furthermore, the disagreement for all values of Λ in the forward hemisphere is even more dramatic.

Note added in proof. [The basic difference between the results of Robinson *et al.*, and those reported here is that this experiment provides an absolute cross section, whereas, in the case of Robinson *et al.*, the experimental points were normalized to obtain a fit to the predicted cross sections.]

To comment first on the forward angle discrepancy: The effect is probably real. All of the comparison data shown in Fig. 6 at 60° and forward lie above the theoretical curves (although not so far above as our own data). The discrepancy might seem to have nothing to do with a ρ-meson coupling, because it lies in the region of relatively small momentum transfer to the nucleon, and McKinley's ρ-meson effects are proportional to the momentum transfer. One might hope that the discrepancy comes as a result of setting $N^{(-)}=0$. This choice was based on a statement by Ball[2] that he obtained $N^{(-)}=4.5\times10^{-3}$, a small value which would only have the effect of raising the theoretical cross sections approximately 2%. $N^{(-)}$ is a function of energy, however. A larger value for $N^{(-)}$ is possible, therefore, but, like nearly any other modification of parameters, this would also have the effect of somewhat altering the angular distribution along with the absolute cross section.

Höhler and Dietz,[16] using the expressions derived by Ball[2] have computed the ρ-meson contribution to the isoscalar photoproduction amplitudes. These calculations proceed from Ball's equations (8.23)–(8.26), in which the authors use a value of 16 for the quantity a, and in which the nucleon form-factors, G_2^v and G_1^v are given by

$$G_1^v(t)=e/2\{[26.9/(22.4-t)]-0.2\},$$

$$G_2^v(t)=2.35e/2M\{[26.9/(22.4-t)]-0.2\},$$

[16] Private communication from Professor G. Höhler of the Karlsruhe Institut für Theoretische Kernphysik. The authors are indebted to Professor Höhler for making available to them the results of his work with K. Dietz and W. Schmidt prior to publication.

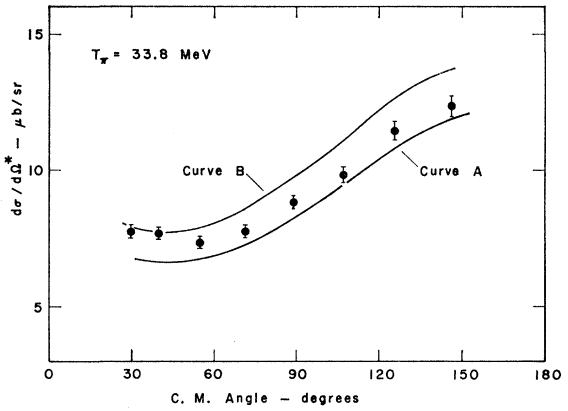

FIG. 9. Comparison of experimental results to calculations of Höhler and Dietz (Ref. 16). Curves are explained in text.

where the units and notation are those of Ball. Figure 9 shows the results of this experiment compared to the results presented by Höhler and Dietz. Curve A is calculated without the inclusion of a ρ-meson coupling, and curve B includes the effect of a ρ-meson coupling with coupling strength $\lambda'=4.3$. (This corresponds to a value of Λ of about 1.) Ball points out that the effect of the ρ meson should be seen at low-momentum transfers, in agreement with curve B, and in disagreement with the predictions shown in Fig. 8.

The discrepancy between the two theoretical predictions concerning the effect on the angular distribution of a resonant two-pion exchange coupled with the other uncertainties (small p-wave phase shifts, electric dipole amplitudes, etc.) in the theory of low-energy photoproduction, leads us to the following conclusion: The data of this experiment, although of sufficient precision to measure the effect of a γ-π-ρ coupling constant Λ of magnitude 0.5 or greater, do not at this time provide a value for Λ because of uncertainties both in the theory of photoproduction and in the measured pion-nucleon scattering parameters.

Further experiments, similar to the one reported here, for photoproduction of charged pions from protons and neutrons are currently being performed at this laboratory.

ACKNOWLEDGMENTS

The authors are indebted to Dr. J. L. Uretsky for early stimulation of this work. L. B. Mortara aided greatly in obtaining the data. R. J. Sprafka was most helpful both in discussing the various theoretical predictions and in performing explicit calculations. To Professor S. Gartenhaus and Paul Finkler we are grateful for useful discussions of the theory of photoproduction.